Linear magnetoresistance in $Ag_{2+\delta}Se$ thin films

M. von Kreutzbruck*
Federal Institute for Materials Research and Testing (Division VIII.4), Unter den Eichen 87, D12205 Berlin, Germany

G. Lembke
Universitätsklinikum Jena, Erlanger Allee 101, D07747 Jena, Germany

B. Mogwitz, C. Korte, and J. Janek
Physikalisch-Chemisches Institut, Justus-Liebig-Universität Gießen, Heinrich-Buff-Ring 58, D-35392 Giessen, Germany

(Received 19 March 2008; revised manuscript received 18 December 2008; published 26 January 2009)

In the nonstoichiometric low-temperature phase of silver selenide a very small silver excess within the semiconducting silver selenide matrix in the order of 0.01% is sufficient to generate a linear magnetoresistance (LMR) of more than 300% at 5 T, which does not saturate at fields up to 60 T. Different theoretical models have been proposed to explain this unusual magnetoresistance (MR) behavior, among them a random resistor network consisting of four-terminal resistor units. According to this model the LMR and the crossover field from linear to quadratic behavior are primarily controlled by both the spatial distribution of the charge-carrier mobility and its average value, being essentially functions of the local and average compositions. Here we report measurements on silver-rich thin Ag_xSe films with a thickness between 20 nm and 2 μm, which show an increasing average mobility in conjunction with an enhanced MR for increasing film thickness. We found a linear scaling between the size of the transverse LMR and the crossover field, as predicted by the theory. For films thinner than about 100 nm the MR with field directed in the sample plane shows a breakdown of the LMR, revealing the physical length scale of the inhomegeneities in thin Ag_xSe devices.

DOI: 10.1103/PhysRevB.79.035204 PACS number(s): 75.47.−m, 72.20.My

In any class of conducting material the relative change in resistance $\Delta\rho/\rho$ in a magnetic field usually is far from linear and saturates at high fields. As exceptions some polycrystalline metals such as potassium or indium show a nonsaturating linear magnetoresistance (MR) (LMR), caused by macroscopic voids or inhomogeneities. This effect is rather small and the linear behavior is only found at large fields of about 1 T,[1,2] so these materials did not stimulate any thoughts of magnetic sensor applications. This changed when a large and nonsaturating LMR was found in Ag_xSe and Ag_xTe with linear characteristics down to 10^{-4} T, leading to intense research activities.[3–8]

The first approach for the explanation of this unusual behavior can be found already several years ago in the theory of Stroud,[9] who calculated the resistance of a two-phase mixture by the resistance of its single components. At certain volume fractions of the components the increase in resistance does not saturate with increasing magnetic field but is linear.[10–12] Other calculations show that the MR also depends strongly on the shape of the conducting inclusions and therewith on the microstructure of the compound.[13–15] Above the percolation threshold, when conducting inclusions in an insulating matrix form a continuous network, the magnetoresistance is asymptotically proportional to the magnetic field.[16] Another theoretical explanation was proposed by Abrikosov[17] as a quantum magnetoresistance for a two-component system with a zero band gap of the semiconducting matrix.

An alternative classical approach reduced on the spatial distribution of the charge-carrier mobility μ and its average value was presented by Parish and Littlewood (PL).[18,19] They found that in a two-dimensional (2D)-random resistor network of four-terminal resistor units an inhomogeneous distribution of μ generally leads to a transversal LMR. In addition the crossover field B_c, marking the transition from quadratic to linear behavior, depends on the mobility distribution, i.e., the microstructure.

Unfortunately the localization of nanosized excess silver clusters or inclusions in bulk samples or films of silver chalcogenides thicker than a few tens of nanometers is impossible by electron imaging techniques without serious damage, and thus, indirect methods are required. Therefore, Hu *et al.*[20] showed in current jetting experiments—measuring a disappearing longitudinal MR for low sample thickness—that the physical length scale λ in bulk samples of $Ag_{2+\delta}Se$ ($-2\times10^{-3}\leq\delta\leq10^{-3}$) is about 10 μm. This length scale gives the dimension of the spatial inhomogeneities in the sample and can be associated directly with the magnetic field strength for the onset of linear response. The obtained 10 μm agree well with the distribution of precipitated silver clusters in $Ag_{2.33}Se$ bulk samples as found experimentally by Beck *et al.*[21] However, when dealing with polycrystalline thin films in inhomogeneous samples of $Ag_{2+\delta}Se$, the physical length scale seems to be smaller than 10 μm, caused by the influence of the smaller grain size of the matrix itself. Recently, high-resolution-transmission-electron-microscopy measurements of 50 nm thick films revealed that a few hundreds of nanometers large silver grains and silver lamellae coexist in the Ag_2Se matrix with an average distance in the order of 1 μm or below. Silver grains and lamellae preferentially start to grow at nonequilibrium lattice defects (primarily along grain boundaries) which act in Ag_xSe as traps for silver atoms.[22–24] Therefore a few vol % of excess silver are sufficient to shape a percolating silver network which increases the conductivity by more than 1 order of magnitude within the interval $0<\delta<0.25$. In the regime $0.25<\delta$

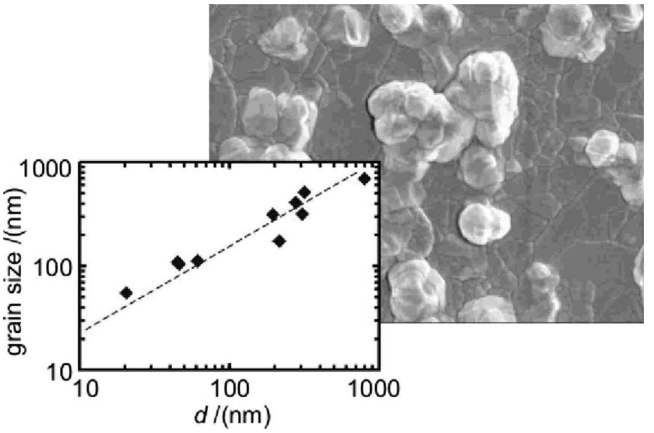

FIG. 1. Scanning electron microscope micrograph of a $Ag_{2.4}Se$ film with a thickness of 730 nm. The surface reveals the grain structure and the crystallites growing out of the plane. Inset: average grain size as a function of the film thickness.

<1.3 the silver paths saturate and any further silver excess causes the growth of metal grains inside the matrix grains as well. These grains appear to be nonconnected and thus have a negligible effect on the conductivity compared to the percolating silver paths along the grain surfaces.[25]

The silver-decorated grain boundaries lead to samples with different average mobility μ. Our Ag_xSe films were fabricated by pulsed laser deposition (PLD) [Kr-F excimer laser ($\lambda=248$ nm, Compex 201)] of stoichiometric silver selenide, which has been prepared by comelting of the elements (99.999% purity). Films with an area of 10×10 mm^2 were deposited on single-crystal MgO substrates at a temperature of 120 °C. The pulse energy was 200 mJ and the repetition rate was 10 Hz. Argon was used as background gas with a pressure of 2 Pa. The distance between target and the substrate was adjusted to be 45 mm. The film thickness and the morphology were determined by high-resolution scanning electron microscopy (Leo Gemini 982). Energy dispersive x-ray analysis (Oxford INCA) was used to study the composition. The resistivity and MR effect of the films were measured by a standard four-probe method using a 17 T superconducting magnet system (Oxford Instruments) with temperature control ranging from 2 to 300 K (Cernox thermometer). The mobility and charge-carrier concentration were determined by measuring the Hall effect using a van der Pauw configuration.

The films start to grow with an average grain diameter about two times larger than the film thickness, which then grows linearly with film thickness (Fig. 1) due to ripening processes at the deposition temperature. As a result the grain size, the corresponding network of grain boundaries (and dislocations), and the electron mobility are a function of the film thickness. A continuous increase in μ is achieved by using samples of varying thickness between 10 nm and 1 μm.

For $d>60$ nm the films exhibit an average resistivity of about 0.4 mΩ cm. Measuring the conductivity, determining the Kohler slope and the temperature dependence, we found that for $d<60$ nm the samples have a higher resistivity of about 0.8 mΩ cm, are not in the percolative regime, and

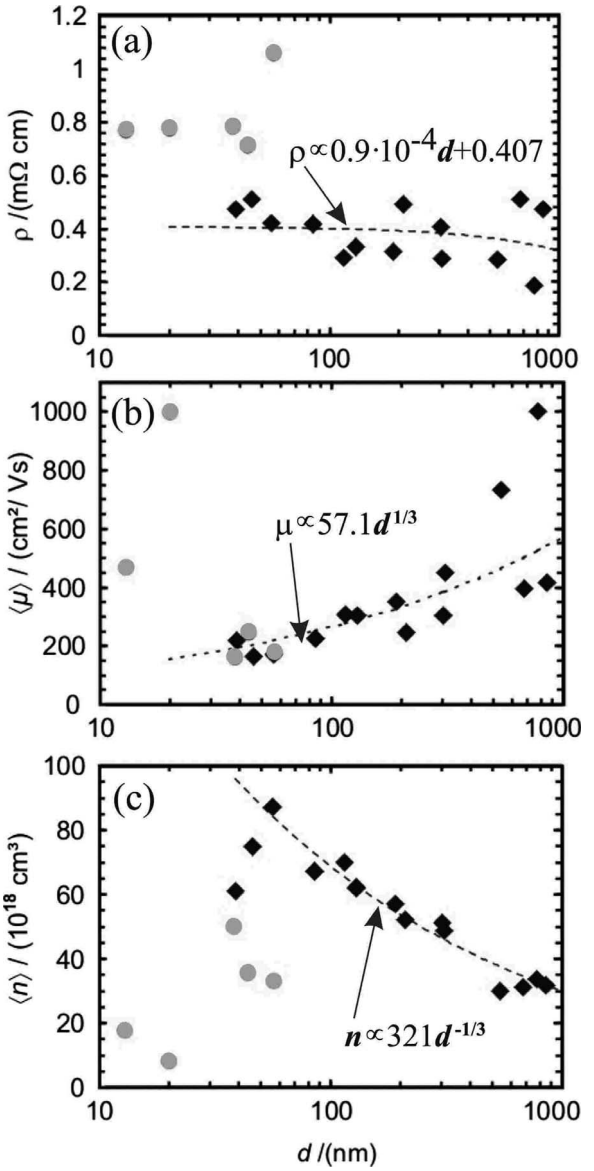

FIG. 2. Electrical properties derived from the Hall effect. Resistance (a), mobility (b), and charge-carrier concentration (c) as a function of the film thickness. The dashed lines correspond to $\rho\propto0.9\times10^{-4}d+0.407$ (a), $n\propto321d^{-1/3}$ (b), and $\mu\propto57.1d^{1/3}$ (c). Gray points: samples which are not in the percolative regime. Black diamonds: samples containing percolating silver paths.

thus show typical semiconducting behavior. The silver network in the semiconductor/metal heterostructure was more reliably characterized by measuring weak localization (WL) effects. These could be observed for films thinner than 300 nm at temperatures of 4.2 K, contributing an increase in resistivity at fields in the order of a few hundreds of millitesla. From the WL data we determined the corresponding characteristic electron-scattering lengths, such as the spin-orbit length L_{SO} and the inelastic length $L_i(T)$. Their ratio differs for percolating and nonpercolating samples by a factor of 6.

The almost constant resistivity of the films (Fig. 2, top) implies a virtually constant product of the average charge-carrier concentration $\langle n\rangle$ and electron mobility $\langle\mu\rangle$. The mobility $\langle\mu\rangle$ of a 40 nm thick sample is about a factor of 3

smaller than for a 1 μm thick sample (Fig. 2, middle). Surprisingly, $\langle n \rangle$ decreases by a factor of 3 for the film thickness between 60 and 600 nm (Fig. 2, bottom). Two superimposed effects can be accounted for this unusual behavior, both depending on the ratio of excess silver being deposited in nonconnected grains or in percolating silver films along grain boundaries. First, decreasing the grain size by reducing the film thickness increases the density of grain-boundary interfaces, in which a larger amount of excess silver can be incorporated. This, in turn, increases $\langle n \rangle$, as charge transport then takes place mainly along the percolating silver paths rather than via single silver grains. Note that the electron mobility of silver is about 2 orders of magnitude smaller than that of Ag_2Se. A larger amount of silver within the percolating current paths therefore leads to a decrease in $\langle \mu \rangle$. However, this influence of the silver excess alone is not sufficient to explain $\langle \mu \rangle$ as a function of the film thickness, as a larger fraction of silver within the silver percolation paths does inevitably enhance the conductivity, which was not observed for the whole thickness range. Second, we have to take into account the internal size effect based on electron scattering at the grain boundaries. This effect is well known for high mobility semiconductors and decreases $\langle \mu \rangle$ of thin films with their smaller grain size in the order of a few tens of nanometers, as observed in Fig. 2 (middle).[26,27] But again, our findings cannot be interpreted with this effect alone, as electron grain-boundary scattering does not explain the increase in the charge-carrier concentration n with decreasing film thickness.

The MR effect of all films was measured for two different alignments between the magnetic field B and the electrical current I: the longitudinal MR_L ($B \| I$) and the transversal MR_T ($B \perp I$). MR_T was determined for both a field aligned parallel [$MR_\|$, $B \perp I$, and $B \| \square$ (film plane)] and perpendicular ($MR_\perp$, $B \perp I$, and $B \perp \square$) to the sample. Films with a thickness of about 1 μm show a $MR_\perp$ of about 200% at $B = 12$ T and $T = 4.2$ K (Fig. 3, top). Higher temperatures yield smaller MR values. The LMR effect decreases linearly with decreasing sample thickness to values of about 50% at $d = 100$ nm. By comparing $MR_\perp$ for $d \leq 85$ nm with the linear approximation $\Delta\rho/\rho_\perp = 0.072d + 55$ [dashed red (gray) line in Fig. 3, top] we observe somewhat smaller MR values than expected. For $d > 85$ nm also $MR_\|$ can be linearly approximated and is about a factor of 3 smaller than $MR_\perp$. Note that Fig. 3 shows the values in a double-logarithmic plot. Remarkably we observe a breakdown of $MR_\|$ to values lower than 2.5% for $d < 85$ nm, which is more than 1 order of magnitude smaller than $MR_\perp$ (Fig. 3, top). Moreover, the longitudinal MR_L is a factor of 2 smaller than its transverse counterpart $MR_\|$ for the total thickness interval (not shown here) also showing the disappearance of the MR for films thinner than 100 nm. The MR data in Fig. 3 (top) scatter significantly, thus indicating that the given physical length scale varies as a result of the PLD preparation process and the statistical character of the microstructure.

As example for the linearity of the MR the normalized $MR_\|$ is shown in Fig. 3 (bottom) as a function of the applied field. The curves are scaled such that they have the same $MR_\|$ at 12 T and show a much more pronounced LMR for thicker films. The crossover field from linear to quadratic

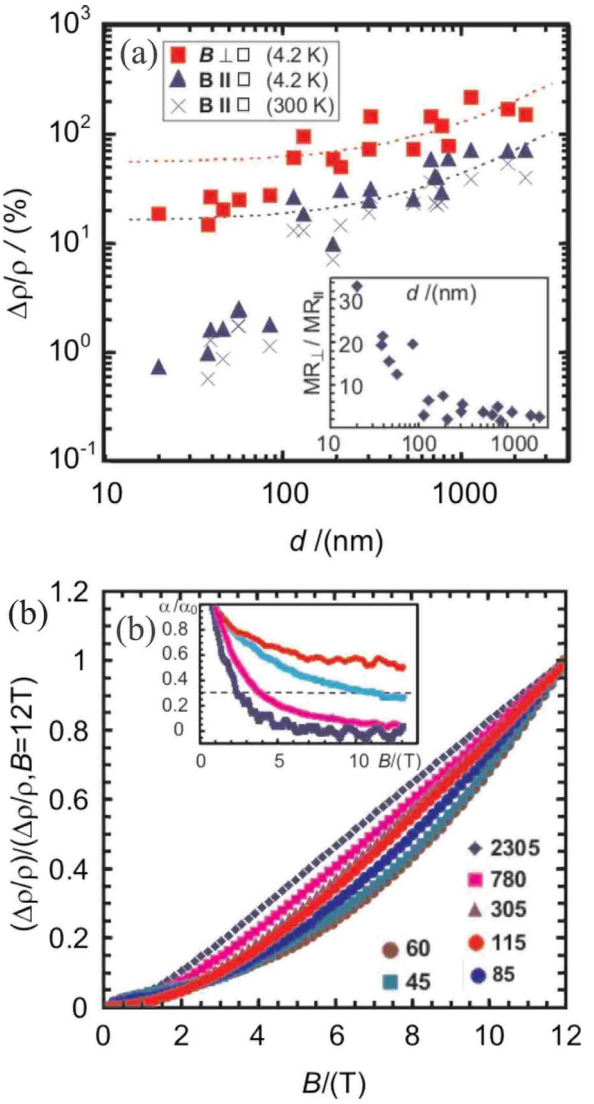

FIG. 3. (Color online) Strength and linearity of the magnetoresistance. (a) Transversal MR as a function of the film thickness for $B = 12$ T. Red (gray) squares: $MR_\perp$ at 4.2 K with field perpendicular to the film [red (gray) dashed line: $\Delta\rho/\rho_\perp = 0.072d + 55$]; blue (black) triangles: $MR_\|$ with field in plane and perpendicular to the current [blue (black) dashed line: $\Delta\rho/\rho_\| = 0.072d + 16$]. Crosses represents $MR_\|$ at 300 K. Inset: ratio of $MR_\perp$ and $MR_\|$ as a function of the film thickness. (b) Normalized $MR_\|$ for 4.2 K as a function of the applied field for different film thicknesses in nm. Inset: determination of the crossover field B_c derived from $MR_\perp$ data and the corresponding quadratic coefficient α for different film thickness [$B_c = B(\alpha/\alpha_0 = 0.3)$, blue (black): 2305 nm, pink (middle gray): 780 nm, green (light gray): 45 nm, and red (dark gray): 20 nm].

MR behavior B_c was determined by the quadratic fit function $\Delta\rho/\rho = \alpha B^2 + \beta B + \gamma$. A vanishing coefficient α indicates linearity and was determined for each 1 T interval in steps of 70 mT up to 14 T. B_c was then defined as the field at which $\alpha/\alpha_0 < 0.3$, where α_0 is the maximum of $\alpha(B)$ at low fields in the quadratic regime (inset of Fig. 3, bottom). Thick samples with $d > 1$ μm yield a B_c in the order of 2 T, which is steadily increased to about 10 T for $d = 100$ nm. Films thinner than 100 nm show even higher crossover fields for

both $MR_{\parallel}$ and $MR_{\perp}$. For $B_c > 14$ T we extrapolated $\alpha/\alpha_0(B)$ up to higher fields where the crossover at $\alpha/\alpha_0 < 0.3$ occurs. It turned out that for $d \leq 85$ nm $MR_{\parallel}$ is far away from the linear regime showing crossover fields well beyond 50 T.

How does these LMR data correspond with the model of Parish and Littlewood (PL)? PL introduced a two-dimensional random resistor network model, where the Hall component could be calculated. One single network resistor unit consists of a homogeneous conducting disk with four terminals located at each 90°. An applied magnetic field aligned perpendicular to the resistor plane leads to a current flow perpendicular to the main current flow from the left electrode to the right contact. The conductivity and the mobility of one resistor unit are randomly determined, which can lead to a complex current distribution. Even a negative local current flow with respect to the main voltage at both contacts was observed. The total $N \times M$ network impedance and the corresponding MR properties were then calculated for a large magnetic field range and for a variety of disorder in terms of local variation in the mobility and conductivity. PL showed that classical disorder is a possible explanation of the LMR of the silver chalcogenides. They found that an inhomogeneous distribution of the mobility μ generally leads to a transversal LMR. In addition it was shown that the crossover field B_c, marking the transition from quadratic to linear behavior, is determined by the mobility distribution, i.e., the microstructure.

Our films within the percolating regime fulfill the condition $\Delta\mu/\langle\mu\rangle < 1$, confirmed by relatively large crossover fields of more than 1 T. Provided we have large fields well beyond B_c, the PL model predicts for this case that $\Delta\rho/\rho \propto \langle\mu\rangle$ and $B_c \propto 1/\langle\mu\rangle$. The model further predicts that the proportionality factor also depends on the length scale λ and the corresponding spatial distribution of the mobility, i.e., on the microstructure of the sample. We thus can describe the proportionality factor as product of a constant and a function of λ,

$$\Delta\rho/\rho = k_1 \cdot f(\lambda) \cdot \langle\mu\rangle. \tag{1}$$

We can safely assume that the influence of the microstructure on the MR and on B_c, generating the scattered data in Fig. 3 (top), is caused by the same physical reason: both $\langle\mu\rangle$ and the degree of disorder with its characteristic physical length scale. We therefore imply the same proportionality factor $f(\lambda)$ for the relation of $1/B_c$ and $\Delta\rho/\rho$ and thus expect to find a linear relation between these quantities which is independent of the microstructure,

$$\frac{1}{B_c} = k_2 \cdot f(\lambda) \cdot \langle\mu\rangle, \quad \frac{\Delta\rho}{\rho} = \frac{k_1}{k_2} \cdot \frac{1}{B_c}. \tag{2}$$

In Fig. 4 MR_T is depicted as a function of the inverse crossover field. The linear scaling of the MR for $B_c < 8$ T, indicated by the dashed lines, indeed confirms Eq. (2) and the corresponding PL model. For $d \leq 85$ nm we can observe again lower MR values compared to the linear approximation. Considering that $B_c > 10$ T for $d \leq 85$ nm, $MR_{\perp}$ is not fully in the linear regime at 12 T leading to smaller MR values. Similarly, for $MR_{\parallel}$, where the breakdown appears, we found extremely large crossover fields of higher than 60 T. This indicates that for the thinnest samples $MR_{\parallel}$ is still completely in the quadratic regime in conjunction with smaller derivatives $\partial(\Delta\rho/\rho)/\partial B$, leading to distinctly smaller MR values at 12 T. This interpretation is supported by an increasing crossover field for decreasing film thickness for $d < 60$ nm in conjunction with a continuously enhanced ratio $MR_{\perp}/MR_{\parallel}$ (inset of Fig. 3, top). We therefore stress that Eq. (2) even holds for a sample thickness down to 20 nm for both $MR_{\parallel}$ and $MR_{\perp}$, provided the MR is measured well beyond B_c. Moreover, the linear behavior of $MR_{\parallel}(d)$, where charge carriers are generally deviated perpendicular to the sample plane, implies that the linear relations of the PL model, derived from polar configuration ($MR_{\perp}$) and 2D systems only, are universal and even hold in three-dimensional (3D) geometries.

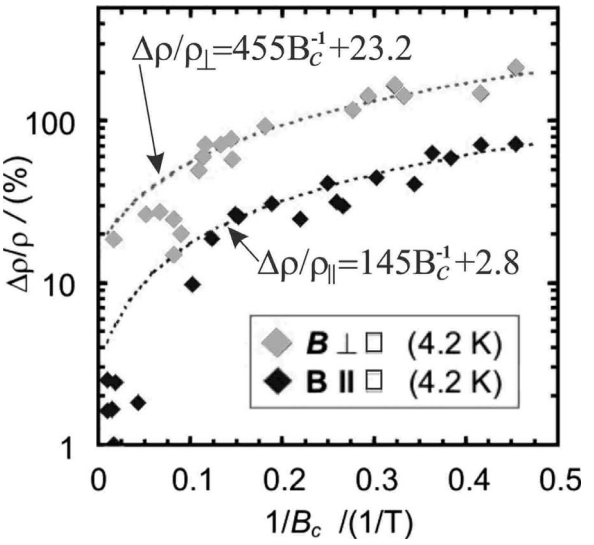

FIG. 4. Magnetoresistance as a function of the inverse crossover field. Transversal magnetoresistance (MR_T, field perpendicular to the current) for $B=12$ T. Gray diamonds: $MR_{\perp}$ at 4.2 K with field perpendicular to the film; black diamonds: $MR_{\parallel}$ at 4.2 K with field in plane. Determined from the data in Fig. 3, we found for $d > 100$ nm B_c values of smaller than 10 T, whereas for $d < 100$ nm B_c is decreased to values up to 20 T for $MR_{\perp}$ and normally higher than 50 T for $MR_{\parallel}$.

As a further result we can extract the physical length scale of the LMR in thin films from the breakdown phenomenon. The breakdown film thickness is close to the average size of the silver precipitates, which was roughly determined from x-ray diffraction studies to be about 130 nm.[28] $MR_{\parallel}$ (and also $MR_{\perp}$) thus disappears when the film thickness becomes of the order of the size of the inhomogeneities. Again, our samples are in the percolating limit for $d > 60$ nm. Considering that Ag and Ag_2Se differ in electrical conductivity by almost 3 orders of magnitude, this is in agreement with the-

oretical findings of a zero MR in a 2D two-component system (where one of the components is basically insulating) and a linear MR in the 3D counterpart.[29] Finally, it is worth mentioning that the average mean-free path (MFP) of electrons in our films is lower than 30 nm. This strengthens the classical approach and indicates that the MFP thus cannot hold as a reason for the breakdown.

A huge extraordinary magnetoresistance (EMR) effect was also reported by Solin *et al.*[30] in a macroscopic circular metallic inclusion in a bulk semiconductor disk made from InSb. It appears that both the LMR as well as the EMR can be explained by classical theories and are geometrical in nature suggesting they might have similar physical reasons.[31] However, in contrast to the LMR effect the EMR shows quadratic field dependence, saturates at high fields, and also occurs in 2D geometry. Although the highest MR at a few tesla was found for macroscopic EMR devices, nanostructured mesoscopic devices with a few hundreds of nanometers in size were proposed as field sensors for read head systems and show competitive properties with respect to established giant magnetoresistance devices.[32] It is yet unclear whether nanostructured LMR films with lateral dimensions in the order of 100 nm can work, as the linear effect may disappear. Further work is required to study the breakdown in low dimensional LMR systems and to explore possible nanoscopic sensor applications. In any case, silver selenide will only be the material of choice in low-temperature applications due to the high chemical diffusion coefficient of silver. With respect to room-temperature applications alternative LMR materials such as the narrow gap semiconductor $LaSb_2$, also showing an intrinsic large, linear, and nonsaturating MR effect,[33,34] might be a promising alternative.

We thank M. Parish for helpful discussions and S. Graubner for assistance with Hall measurements. Support by Deutsche Forschungsgemeinschaft is gratefully acknowledged.

*marc.kreutzbruck@bam.de

[1] J. Babiskin and P. G. Siebenmann, Phys. Rev. Lett. **27**, 1361 (1971).
[2] C. J. Beers, J. C. M. vanDongen, H. vanKempen, and P. Wyder, Phys. Rev. Lett. **40**, 1194 (1978).
[3] R. Xu, A. Hussmann, T. F. Rosenbaum, M.-L. Saboungi, J. E. Enderbya, and P. B. Littlewood, Nature (London) **390**, 57 (1997).
[4] M. Lee, T. F. Rosenbaum, M. L. Saboungi, and H. S. Schnyders, Phys. Rev. Lett. **88**, 066602 (2002).
[5] H. S. Schnyders, M.-L. Saboungi, and T. F. Rosenbaum, Appl. Phys. Lett. **76**, 1710 (2000).
[6] A. Husmann, J. B. Betts, G. S. Boebinger, A. Migliori, T. F. Rosenbaum, and M.-L. Saboungi, Nature (London) **417**, 421 (2002).
[7] S. S. Manoharan, S. J. Prasanna, D. Elefant-Kiwitz, and C. M. Schneider, Phys. Rev. B **63**, 212405 (2001).
[8] Z. Ogorelec, A. Hamzic, and M. Basletic, Europhys. Lett. **46**, 56 (1999).
[9] D. Stroud, Phys. Rev. B **12**, 3368 (1975).
[10] V. Guttal and D. Stroud, Phys. Rev. B **73**, 085202 (2006).
[11] S. A. Bulgadaev and F. V. Kusmartsev, Phys. Lett. A **342**, 188 (2005).
[12] R. Magier and D. J. Bergman, Phys. Rev. B **74**, 094423 (2006).
[13] D. J. Bergman and Y. M. Strelniker, Phys. Rev. B **49**, 16256 (1994).
[14] D. J. Bergman and Y. M. Strelniker, Phys. Rev. B **59**, 2180 (1999).
[15] D. J. Bergman and Y. M. Strelniker, Phys. Rev. B **60**, 13016 (1999).
[16] D. J. Bergman and D. G. Stroud, Phys. Rev. B **62**, 6603 (2000).
[17] A. A. Abrikosov, Phys. Rev. B **58**, 2788 (1998).
[18] M. M. Parish and P. B. Littlewood, Nature (London) **426**, 162 (2003).
[19] M. M. Parish and P. B. Littlewood, Phys. Rev. B **72**, 094417 (2005).
[20] J. Hu, T. F. Rosenbaum, and J. B. Betts, Phys. Rev. Lett. **95**, 186603 (2005).
[21] G. Beck, C. Korte, F. Gruhl, and M. Kreutzbruck, J. Appl. Phys. **96**, 5619 (2004).
[22] Y. Kumashiro, T. Ohachi, and T. Taniguchi, Solid State Ionics **86-88**, 761 (1996).
[23] T. Ohachi, M. Hiramoto, Y. Yoshihara, and I. Taniguchi, Solid State Ionics **51**, 191 (1992).
[24] J. Janek, B. Mogwitz, G. Beck, M. Kreutzbruck, and L. Kienle, Prog. Solid State Chem. **32**, 179 (2004).
[25] M. von Kreutzbruck, B. Mogwitz, F. Gruhl, L. Kienle, C. Korte, and J. Janek, Appl. Phys. Lett. **86**, 072102 (2005).
[26] K. Kanisawa, H. Yamaguchi, and Y. Hirayama, Appl. Phys. Lett. **76**, 589 (2000).
[27] E. Michel, G. Singh, S. Slivken, C. Besikci, P. Bove, I. Ferguson, and M. Razeghi, Appl. Phys. Lett. **65**, 3338 (1994).
[28] B. Mogwitz, C. Korte, M. Kreutzbruck, and L. Kienle, J. Appl. Phys. **101**, 043510 (2007).
[29] J. Hu, M. Parish, and T. F. Rosenbaum, Phys. Rev. B **75**, 214203 (2007).
[30] S. A. Solin, Tineke Thio, D. R. Hines, and J. J. Heremans, Science **289**, 1530 (2000).
[31] W. R. Branford, A. Husmann, S. A. Solin, S. K. Clowes, T. Zhang, Y. V. Bugoslavsky, and L. F. Cohen, Appl. Phys. Lett. **86**, 202116 (2005).
[32] S. A. Solin, D. R. Hines, A. C. H. Rowe, J. S. Tsai, Yu. A. Pashkin, S. J. Chung, N. Goel, and M. B. Santos, Appl. Phys. Lett. **80**, 4012 (2002).
[33] D. P. Young, R. G. Goodrich, J. F. DiTusa, S. Guo, P. W. Adams, J. Y. Chan, and D. Hall, Appl. Phys. Lett. **82**, 3713 (2003).
[34] R. G. Goodrich, D. Browne, R. Kurtz, R. Young, J. F. DiTusa, P. W. Adams, and D. Hall, Phys. Rev. B **69**, 125114 (2004).